

HIGH SPATIAL RESOLUTION T-RECS MID-INFRARED IMAGING OF LUMINOUS INFRARED GALAXIES

ALMUDENA ALONSO-HERRERO¹, LUIS COLINA¹, CHRISTOPHER PACKHAM², TANIO DÍAZ-SANTOS¹, GEORGE H. RIEKE³,
JAMES T. RADOMSKI⁴, AND CHARLES M. TELESCO³

Draft version March 23, 2021

ABSTRACT

We present diffraction-limited (FWHM $\sim 0.3''$) Gemini/T-ReCS mid-infrared (MIR: N -band or narrow-band at $8.7\ \mu\text{m}$) imaging of four Luminous Infrared Galaxies (LIRGs) drawn from a representative local sample. The MIR emission in the central few kpc is strikingly similar to that traced by Pa α , and generally consists of bright nuclear emission and several compact circumnuclear and/or extranuclear H II regions. The central MIR emission is dominated by these powerful H II regions, consistent with the majority of AGN in this local sample of LIRGs contributing a minor part of the MIR emission. The luminous circumnuclear H II regions detected in LIRGs follow the extrapolation of the $8\ \mu\text{m}$ vs. Pa α relation found for M51 H II knots. The integrated central 3 – 7 kpc of galaxies, however, present elevated $8\ \mu\text{m}/\text{Pa}\alpha$ ratios with respect to individual H II regions, similar to the integrated values for star-forming galaxies. Our results show that the diffuse $8\ \mu\text{m}$ emission, not directly related to the ionizing stellar population, can be as luminous as that from the resolved H II regions. Therefore, calibrations of the star formation rate for distant galaxies should be based on the integrated $8\ \mu\text{m}$ emission of nearby galaxies, not that of the H II regions alone.

Subject headings: galaxies: evolution — galaxies: nuclei — galaxies: Seyfert — galaxies: structure — infrared: galaxies

1. INTRODUCTION

There is growing interest in using the mid-infrared (MIR) emission of infrared (IR) selected distant galaxies as an indicator of the massive and dusty star formation rate (SFR), analogously to the widely used SFR vs. IR calibration of Kennicutt (1998). The unprecedented sensitivity provided by *Spitzer* observations reveals the good overall morphological correspondence between the ionized gas (i.e., H α , Pa α) and the MIR ($8 - 24\ \mu\text{m}$) emission of nearby galaxies (Helou et al. 2004; Hinz et al. 2004; Gordon et al. 2004; Calzetti et al. 2005, CAL05 hereafter). This suggests that the MIR emission could be used as an accurate SFR indicator, especially for dusty galaxies. For instance, CAL05 and Alonso-Herrero et al. (2006, AAH06 hereafter) for resolved H II knots in M51 and for local Luminous Infrared Galaxies (LIRGs⁵) respectively, found that the $24\ \mu\text{m}$ continuum emission is a good local SFR indicator (see also Wu et al. 2005). CAL05 and Pérez-González et al. (2006) questioned the use of the IRAC $8\ \mu\text{m}$ continuum emission based on the larger scatter of the $8\ \mu\text{m}$ vs. H α (or Pa α) relation for resolved H II regions in nearby galaxies, whereas Wu et al. (2005) found a good correlation for local star-forming galaxies. This demonstrates the need for further investigation of this issue.

Although *Spitzer* provides highly sensitive imaging of LIRGs (Mazzarella et al. 2005), it cannot resolve the

sizes of the MIR emitting regions. We present the results of a pilot study intended to understand the MIR properties of LIRGs at high spatial resolution (tens-hundreds of parsecs), using the Thermal-Region Camera Spectrograph (T-ReCS; Telesco et al. 1998) on the 8.1 m Gemini-South Telescope. We observed four LIRGs from the representative sample of 30 local ($z < 0.017$) LIRGs of AAH06 which was drawn from the *IRAS* Revised Bright Galaxy Sample (RBGS, Sanders et al. 2003) such that the Pa α ($\lambda_{\text{rest}} = 1.876\ \mu\text{m}$) emission line could be observed with NICMOS on the *Hubble Space Telescope* (HST). Gemini/T-ReCS and the NICMOS NIC2 camera provide comparable spatial resolutions, $\sim 0.30''$ and $\sim 0.15''$, respectively, making them ideal for this kind of study. Throughout this paper we use $H_0 = 75\ \text{km s}^{-1}\ \text{Mpc}^{-1}$, $\Omega_M = 0.3$, and $\Omega_\Lambda = 0.7$.

2. T-RECS MIR IMAGING OBSERVATIONS

We obtained imaging observations of four LIRGs using T-ReCS in September 2005, and March-April 2006. T-ReCS has a plate scale of $0.089''\text{pixel}^{-1}$ which results in a field of view (FOV) of $\sim 28.5'' \times 21.4''$. Three LIRGs (NGC 5135, IC 4518W, and NCG 7130) were observed with the broad-band filter N (central wavelength $\lambda_c = 10.36\ \mu\text{m}$ and width at 50% cut-on/off $\Delta\lambda = 5.27\ \mu\text{m}$) and NGC 3256 with the narrow-band Si-2 filter ($\lambda_c = 8.74\ \mu\text{m}$, and $\Delta\lambda = 0.78\ \mu\text{m}$). The on-source integration times were NGC 3256: 304s, NGC 5135 and NGC 7130: 608s, and IC 4518W: 1216s. Packham et al. (2005) described the observation procedures and data reduction. The uncertainties of the photometric calibration were 5 – 15%. The standard star FWHMs ($\sim 0.30''$, Table 1) indicate that the T-ReCS observations were effectively diffraction limited, implying spatial resolutions of $\sim 50 - 100\ \text{pc}$ for our LIRGs. For details on the *HST*/NICMOS data reduction see AAH06. The T-ReCS and *HST*/NICMOS images are presented in Fig. 1.

¹ Departamento de Astrofísica Molecular e Infrarroja, Instituto de Estructura de la Materia, CSIC, E-28006 Madrid, Spain; aalonso, colina, tanio@damir.iem.csic.es

² Department of Astronomy, University of Florida, 211 Bryant Science Center, P.O. Box 112055, Gainesville, FL 32611-2055; packham, telesco@astro.ufl.edu

³ Steward Observatory, University of Arizona, 933 N. Cherry Avenue, Tucson, AZ 85721; grieke@as.arizona.edu

⁴ Gemini Observatory, c/o AURA, Casilla 603, La Serena, Chile; jradomski@gemini.edu

⁵ $L_{\text{IR}[8-1000\ \mu\text{m}]} = 10^{11} - 10^{12}\ L_\odot$, see Sanders & Mirabel (1996).

TABLE 1
 PHOTOMETRY.

Galaxy	Class	Dist. (Mpc)	$\log L_{\text{IR}}$ (L_{\odot})	$f_{\nu}(12\ \mu\text{m})$ (mJy)	TReCS FWHM		NICMOS FWHM		T-ReCS f_{ν}			IRAC $f_{\nu}(8\ \mu\text{m})$		
					star (")	nuclear (")	nuclear (")	nuclear (pc)	nucleus	5'' (mJy)	10''	5''	10''	19'' \times 19'' (mJy)
NGC 3256	HII	35	11.56	3570	0.30	0.45 (N)	0.40 (N)	69 (N)	230 \pm 11 (N)	575 \pm 30	845 \pm 150	462	1399	2436
	HII					0.45 (S)	0.40 (S)	69 (S)	40 \pm 3 (S)					
NGC 5135	Sy2	52	11.17	630	0.31	0.35	0.16	\leq 40	80* \pm 3	243 \pm 20	313 \pm 60	214*	408	490
IC 4518W	Sy2	70	11.13**	360**	0.33	0.36	0.15	\leq 51	117* \pm 6	165 \pm 11	–	154*	167*	192
NGC 7130	L/Sy	66	11.35	580	0.31	0.45	0.60	190	130 \pm 6	205 \pm 10	255 \pm 40	148*	232*	372

Notes.— Column (1): Galaxy. Column (2): Activity from optical spectroscopy (see AAH06 for references). Columns (3), (4), and (5): Distance, IR 8 – 1000 μm luminosity, and *IRAS* 12 μm flux density from Sanders et al. (2003). Columns (6), and (7): T-ReCS FWHM of the standard stars, and nuclei. Columns (8) and (9): FWHM from the continuum NICMOS images of the nucleus in arcsec and parsec, respectively. Column (10): nuclear (narrow-band 8.7 μm or *N*-band, see §2) T-ReCS flux density. For the resolved sources the flux density is for a 1.4''-diameter aperture. Columns (11) and (12): T-ReCS flux densities for 5''- and 10''-diameter apertures. The errors only account for the background estimate uncertainties. Columns (13), (14), and (15): IRAC 8 μm flux densities for 5''- and 10''-diameter apertures, and the NICMOS FOV (no aperture corrections have been applied for extended emission).

*: Aperture correction for unresolved emission applied.

** : The *IRAS* 12 μm density flux and IR luminosity are for both the E and W components of IC 4518.

For the nuclei of NGC 3256 and NGC 7130 as well as for the high surface brightness regions (assumed to be H II regions) clearly resolved in the T-ReCS images, we performed aperture photometry. The determination of the underlying background introduces typical MIR photometry uncertainties of 5 – 20%, depending on the brightness of the source. For the unresolved sources (nuclei of NGC 5135 and IC 4518W) the aperture corrections to include all the flux from the point source were computed from standard star observations.

To compare our T-ReCS data with other galaxies (see §3.3), we converted the T-ReCS *N*-band flux densities to IRAC 8 μm ones, convolving *Spitzer*/IRS spectra with the appropriate filter transmissions. For NGC 5135 and NGC 7130 we found $f_{\nu}(\text{IRAC } 8\ \mu\text{m})/f_{\nu}(\text{N-band}) = 0.86$ and 0.76, respectively. These might be average values as spatial variations of the MIR spectral properties of the central regions have been observed in nearby galaxies (e.g., Smith et al. 2004). For the Seyfert (Sy) nuclei of NGC 5135 and IC 4518W, and using a 'generic' IRS Sy2 template (Mrk 3, Weedman et al. 2005), we obtained $f_{\nu}(\text{IRAC } 8\ \mu\text{m})/f_{\nu}(\text{N-band}) = 0.56$. This ratio varies by up to 0.1dex in Sy galaxies observed by IRS (Buchanan et al. 2006). The T-ReCS 8.7 μm flux densities of NGC 3256 are approximately equivalent to the IRAC 8 μm ones. We also performed aperture photometry on the IRAC 8 μm images (Table 1) which have a spatial resolution of 2'' (Fazio et al. 2004).

3. RESULTS AND DISCUSSION

3.1. MIR Structure on scales of tens-hundreds of parsecs

The morphological resemblance (see Fig. 1) between the MIR continuum emitting regions and the H II regions (traced by the Pa α emission) on scales of tens-hundreds of pc in LIRGs (see also Soifer et al. 2001) is remarkable. The near-IR (NIR) continuum emission on the other hand is more extended than the MIR emission (see Keto et al. 1997), and generally does not resemble the morphology of the ionized gas (see AAH06). As $A_{1.6\ \mu\text{m}} \sim 3.3 \times A_N$ (Rieke & Lebofsky 1985), the lack of correspondence between the NIR and MIR (and Pa α) emitting regions is probably not a differential extinction effect. Rather, this may reflect age differences since the NIR continuum is produced mostly by stellar populations older than the ionizing stellar populations (see e.g.,

Alonso-Herrero et al. 2002 and Díaz-Santos et al. 2006), even though highly obscured regions tend to be associated with the youngest regions in LIRGs (Soifer et al. 2001; Díaz-Santos et al. 2006).

The nuclei are the brightest MIR sources in all the galaxies. The Sy2 nuclei of NGC 5135 and IC 4518W⁶ appear unresolved in the MIR (see Table 1), and this is confirmed by the detection of nuclear point sources (Table 1, and also AAH06) in the NICMOS continuum images. The nucleus of NGC 7130 (classified as a Sy or LINER) appears marginally resolved in the T-ReCS images, and the NICMOS continuum images reveal the presence of at least three sources of similar flux in the central \sim 190 pc. This suggests that the putative AGN in NGC 7130 does not dominate (see §3.2) the *N*-band nuclear emission.

NGC 3256 is a well-studied merger galaxy, with two bright nuclei (north and south, see Fig. 2 for location). Kotilainen et al. (1996) and Neff, Ulvestad, & Campion (2003) suggested that the nuclei may host low luminosity AGN. The NIR (Lípari et al. 2000), X-ray (Lira et al. 2002), and MIR spectroscopic (see Martín-Hernández et al. 2006) properties of both nuclei are generally consistent with star formation. The extended (FWHM \sim 60 pc) nature of the NIR and MIR continuum emission of both nuclei further corroborates that such AGN, if present, are not dominant in the MIR.

3.2. AGN Contribution to MIR Emission of LIRGs

Approximately 25% of local LIRGs host spectroscopically confirmed AGN (Veilleux et al. 1995; Goldader et al. 1997; Tran et al. 2001; see Table 1 for our LIRGs). The Sy2 nucleus of NGC 5135 contributes \sim 20% of the *N*-band emission within the central 10'', and even less to the *IRAS* integrated galaxy emission (Table 1). The AGN nucleus of NGC 7130, undetected as a point source, is responsible for $<$ 20% of the total MIR emission (see Table 1). The MIR emission of IC 4518W is dominated by the Sy2 nucleus which accounts for up to \sim 75% (Table 1) of the *N*-band flux density of this galaxy and approximately half of the MIR emission of the system

⁶ There are two Pa α sources oriented north-south in the central region of IC 4518W. The Sy nucleus, the brightest Pa α source and the dominant continuum source at $\lambda \geq 1.6\ \mu\text{m}$, is the south one.

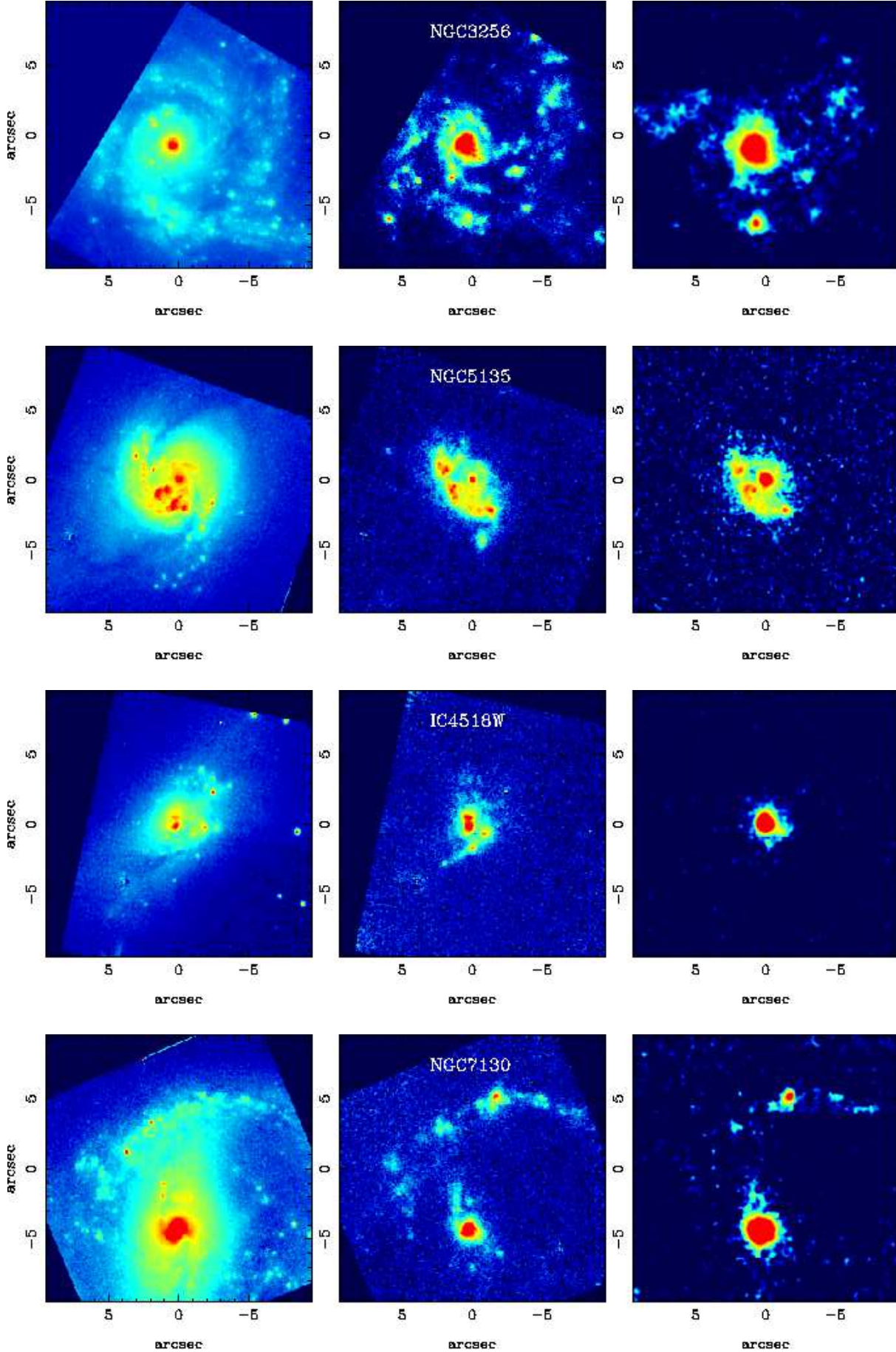


FIG. 1.— *Left panels:* *HST*/NICMOS 1.1 μm continuum emission images except for NGC 3256 which is at 1.6 μm . *Middle panels:* *HST*/NICMOS continuum-subtracted Pa α line emission. The *HST* images except those of NGC 3256 (see Alonso-Herrero et al. 2002) are from AAH06. *Right panels:* Gemini/T-ReCS *N*-band images, except for NGC 3256 which is the narrow-band 8.7 μm filter, for approximately

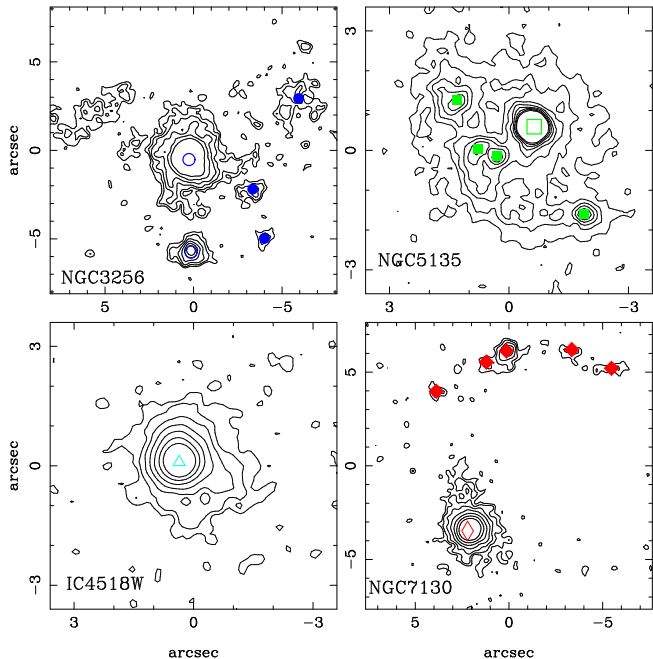


FIG. 2.— The T-ReCS MIR emission contour plots in a logarithmic scale except for NGC 5135 for which the scale is linear. Orientation is north up, east to the left. For each galaxy, the open symbols mark the nuclei, whereas the filled symbols indicate the positions of high surface brightness regions for which photometry was obtained (see also Fig. 3). For NGC 3256 we mark the locations of the north and south nuclei, also detected at NIR (Kolitainen et al. 1996) and radio (Neff et al. 2003) wavelengths.

(IC 4518W+E).

Three more galaxies in the LIRG sample of AAH06, not observed with T-ReCS, have spectroscopically confirmed Sy nuclei. For two of them, the B1 nucleus of the IC 694/NGC 3690 (Arp 299) system (García-Marín et al. 2006), and NGC 7469, the AGN contribution to the MIR emission is $\sim 30\%$ (Keto et al. 1997; Genzel et al. 1995; Soifer et al. 2003). For the third one, there is no MIR information. Our results are consistent with the majority of AGN in our local LIRGs not dominating the MIR emission.

3.3. The 8 – 10 μm MIR Emission as a SFR Indicator?

Deep surveys at 24 μm with *Spitzer* are detecting a large number of LIRGs at $z \sim 1$ and above. These LIRGs contribute significantly to the cosmic SFR density and IR background at $z \sim 1$ (Le Flocc’h et al. 2005; Lagache, Puget, & Dole 2005; Pérez-González et al. 2005). Since the observed 24 μm flux densities translate into rest-frame 8 μm ones at $z = 2$, it is important to assess the accuracy of the MIR-based SFR indicators. A number of works (e.g., CAL05; Pérez-González et al. 2006) find that the rest-frame 8 μm (only dust-emission) monochromatic luminosity is not as tightly correlated with the number of ionizing photons as the 24 μm emission (c.f., Wu et al. 2005).

We further explore the Pa α vs. 8 μm relation in Fig. 3. The LIRG Pa α and MIR emissions are corrected for extinction using the Rieke & Lebofsky (1985) extinction law, and the A_V averaged over the central emitting regions (AAH06). For the nuclei of NGC 3256, we used the

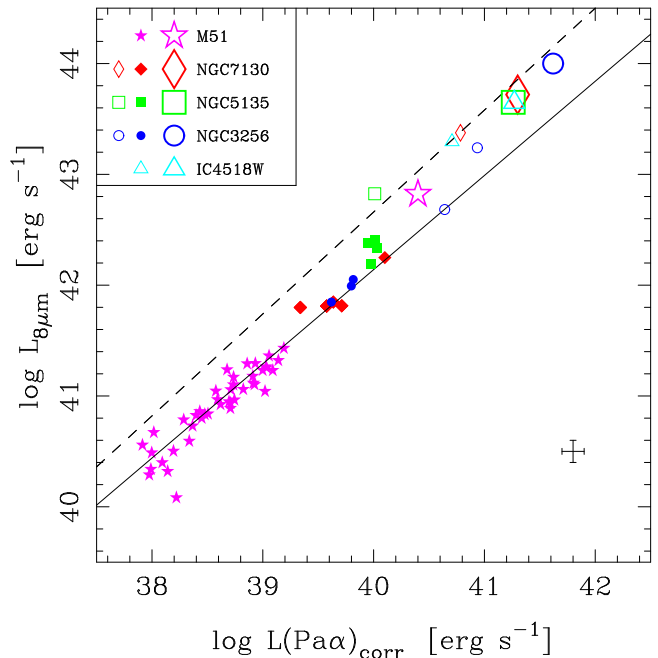


FIG. 3.— Monochromatic (νf_ν) 8 μm vs. extinction-corrected Pa α luminosities. The small open and filled symbols are the nuclei and high surface brightness H II regions (see Fig. 2) of LIRGs, respectively. The photometry for NGC 3256 and NGC 7130 is through a 1.4'' (240 pc and 440 pc respectively) diameter aperture. Crowding effects are likely to be present for the photometry of the circumnuclear H II regions of NGC 5135, even for the 1.1'' (270 pc) aperture used. The error bar indicates the typical uncertainties associated with the photometry and the T-ReCS to IRAC flux density conversion (see §2). The large open symbols for the LIRGs indicate the integrated properties over the *HST*/NICMOS FOV ($\sim 19'' \times 19''$). The central 6 kpc M51 H II regions (photometry for ~ 520 pc diameter apertures) and integrated emission from Calzetti et al. (2005) are shown as star symbols. The IRAC 8 μm photometry is corrected for extended source emission as described by Pérez-González et al. (2006). The solid line is our least-squares fit to the M51 H II region data from Calzetti et al. (2005) extrapolated to the LIRG luminosities. The dashed line is the non-linear fit from Wu et al. (2005) for star-forming galaxies where the H α luminosities have been converted to Pa α ones assuming case B recombination.

nuclear A_V . We assumed that the stellar emission contribution at 8 μm is negligible for our LIRGs. As can be seen from Fig. 3, although the LIRG H II regions are up to 10 times more luminous than those in M51, they tend to follow the extrapolation of the CAL05 relation. Conversely, the integrated $\sim 3 - 7$ kpc emission of LIRGs deviates significantly from the relation found for individual H II regions, but only slightly from the fit of Wu et al. (2005) for star-forming galaxies (Fig. 3). This could arise from two causes. First, Wu et al. (2005) may have underestimated the reddening (obtained from the Balmer decrements) in these dusty star-forming galaxies. Second, the 8 μm emission may be dominated by diffuse emission not associated directly with the H II regions (see below).

The LIRG nuclei (except the south nucleus of NGC 3256) show elevated MIR/Pa α ratios when compared to H II regions. Such spatial differences in the MIR emission of nuclear and circumnuclear regions of nearby galaxies have also been observed (e.g., Smith et al. 2004). One possibility is that an insufficient extinction correction (as nuclear extinctions in LIRGs tend to

be higher than in extranuclear regions) will produce a differential effect, making the nuclei appear more MIR-luminous. The AGN present in three of our LIRGs may also play a role, as their continua are produced by dust heated to higher temperatures than H II regions, and do not present the strong PAH emission characteristic of H II+photodissociation regions (e.g., Laurent et al. 2000; Roche et al. 2006).

The similar behavior of the $8\mu\text{m}$ vs. $\text{Pa}\alpha$ relation for a variety of H II regions in M51 and LIRGs suggests that the $8\mu\text{m}$ emission is well characterized by a thermal continuum plus PAH features with no strong variations over the range of conditions probed here (e.g., metallicity near or over solar, see AAH06 and CAL05). However, the integrated central 3 – 7 kpc $8\mu\text{m}$ vs. $\text{Pa}\alpha$ emission differs significantly in all these environments from the relation found for the individual H II regions. This may be explained by the presence, in addition to the bright and compact H II regions, of a more diffuse and extended $8\mu\text{m}$ component (see Figs. 1 and 2, and Helou et al. 2004). This extra emission at $8\mu\text{m}$ would be produced not by local, strong ionizing sources, but by the diffuse radiation field (see e.g., Tacconi-Garman et al. 2005) that permeates the ISM. As such, the spectrum in these regions would be characterized by a weak continuum and strong PAH features with a large equivalent width. Hence when compared to individual H II regions, an excess of $8\mu\text{m}/\text{Pa}\alpha$ emission can be expected for the integrated properties over a few kpc. This is supported by the fact that the central 3 – 7 kpc emission of LIRGs falls only slightly below the $\text{H}\alpha$ vs. $8\mu\text{m}$ relation found for the integrated properties of the galaxies studied by Wu et al. (2005), as indicated in Fig. 3. For a galaxy with $L_{8\mu\text{m}} = 10^{43} \text{ erg s}^{-1}$, the $8\mu\text{m}$ vs. $\text{Pa}\alpha$ relation for H II regions alone predicts $L(\text{Pa}\alpha)$ (and thus SFR) a fac-

tor of 3 – 4 larger than that given by the relation found for the integrated properties of nearby galaxies.

4. SUMMARY

The N -band (also, the narrow-band at $8.7\mu\text{m}$) emission of local LIRGs resembles the nuclear and H II region emission, as traced by $\text{Pa}\alpha$, on scales of tens-hundreds of parsecs. The AGN contribution to the observed MIR emission in our sample of LIRGs is generally small ($< 20 - 30\%$). The luminous circumnuclear H II regions of LIRGs provide evidence that the $8\mu\text{m}$ vs. $\text{Pa}\alpha$ relation found for M51 knots by CAL05 may extend for a further order of magnitude. The central 3 – 7 kpc regions of LIRGs present elevated $8\mu\text{m}/\text{Pa}\alpha$ ratios with respect to individual H II regions, but similar to those of star-forming galaxies (see Wu et al. 2005). This is probably due to the presence of an extended, diffuse $8\mu\text{m}$ component not directly related to the ionizing stellar population. A better understanding of the $\text{Pa}\alpha$ (or $\text{H}\alpha$) vs. $8\mu\text{m}$ relation for larger samples of nearby star-forming galaxies and LIRGs is required before using the IRAC $8\mu\text{m}$ emission as a SFR tracer for IR-selected high- z galaxies.

Support was provided by the Spanish PNE (ESP2005-01480) and the NSF (0206617). Based on observations obtained at the Gemini Observatory, which is operated by AURA, Inc., under a cooperative agreement with the NSF on behalf of the Gemini partnership: NSF (USA), PPARC (UK), NRC (Canada), CONICYT (Chile), ARC (Australia), CNPq (Brazil) and CONICET (Argentina). Based on observations with the NASA/ESA *HST*, obtained at the STScI, which is operated by AURA, Inc., under NASA contract NAS 5-26555.

REFERENCES

- Alonso-Herrero, A., et al. 2002, *AJ*, 124, 166
 Alonso-Herrero, A., et al. 2006, *ApJ*, 650, 835 (AAH06)
 Buchanan, C. L. et al. 2006, *AJ*, 132, 401
 Calzetti, D., et al. 2005, *ApJ*, 633, 871 (CAL05)
 Díaz-Santos, T., et al. 2006, *ApJ*, submitted
 Fazio, G. G., et al. 2004, *ApJS*, 154, 10
 García-Marín, M., et al. 2006, *ApJ*, 650, 850
 Genzel, R., et al. 1995, *ApJ*, 444, 129
 Goldader, J. D., et al. 1997, *ApJ*, 474, 104
 Gordon, K. D., et al. 2004, *ApJS*, 154, 215
 Helou, G., et al. 2004, *ApJS*, 154, 253
 Hinz, J. L., et al. 2004, *ApJS*, 154, 259
 Kennicutt, R. C. Jr. 1998, *ARA&A*, 36, 189
 Keto, E., et al. 1997, *ApJ*, 485, 598
 Kotilainen, J. K., et al. 1996, *A&A*, 305, 107
 Lagache, G., Puget, J.-L., & Dole, H. 2005, *ARA&A*, 43, 727
 Laurent, O., et al. 2000, *A&A*, 359, 887
 Le Floch, E., et al. 2005, *ApJ*, 632, 169
 Lípári, S., et al. 2000, *AJ*, 120, 645
 Lira, P., et al. 2002, *MNRAS*, 330, 259
 Martín-Hernández, N. L., et al. 2006, *A&A*, 455, 853
 Mazzarella, J. M., et al. 2005, *AAS*, 207, 2106
 Neff, S. G., Ulvestad, J. S., & Campion, S. D. 2003, *ApJ*, 599, 1043
 Packham, C., et al. 2005, *ApJ*, 618, L17
 Pérez-González, P. G., et al. 2005, *ApJ*, 630, 82
 Pérez-González, P. G., et al. 2006, *ApJ*, 648, 987
 Rieke, G. H., & Lebofsky, M. J. 1985, *ApJ*, 288, 618
 Roche, P. F., et al. 2006, *MNRAS*, 367, 1689
 Sanders, D. B., & Mirabel, I. F. 1996, *ARA&A*, 34, 749
 Sanders, D. B., et al. 2003, *AJ*, 126, 1607
 Smith, J. D. T., et al. 2004, *ApJS*, 154, 199
 Soifer, B. T., et al. 2001, *AJ*, 122, 1213
 Soifer, B. T., et al. 2003, *AJ*, 126, 143
 Tacconi-Garman, L. E., et al. 2005, *A&A*, 432, 91
 Telesco, C. M., et al. 1998, *Proc. SPIE*, 3354, 534
 Tran, Q. D., et al. 2001, *ApJ*, 552, 527
 Veilleux, S., et al. 1995, *ApJS*, 98, 171
 Weedman, D. W., et al. 2005, *ApJ*, 633, 706
 Wu, H., et al. 2005, *ApJ*, 632, L79